Iranian Journal of Geophysics, Vol 18 No 6, 2025, Page 112 – 128 (Research Article)
DOI: 10.30499/ijg.2024.445644.1579

Insights from the 2017 and 2020 M_w ~5 earthquakes around Tehran: Assessing seismicity and physical and social vulnerability

Mohammadreza Jamalreyhani [1*], Afshar Hatami[2], MirAli Hassanzadeh[3], Pınar Büyükakpınar[4], Ramin Movaghari [1]

[1]Ph.D., Southern University of Science and Technology, Shenzhen, China
[2] Ph.D., University of Kharazmi, Tehran, Iran
[3]Ph.D., Institute for Advanced Studies in Basic Sciences (IASBS), Department of Earth Sciences, Zanjan, Iran
[4]Associate Professor, GFZ German Research Centre for Geosciences, German, Potsdam

(Received: 25 February 2024, Accepted: 10 July 2024)

Abstract

Tehran is one of the most earthquake-prone cities globally. This vast urban center, with a population exceeding 10 million, is intersected by several active faults, presenting significant seismic hazards. The occurrence of two M_w ~5 earthquakes in December 2017 near Malard and May 2020 near Damavand, further underscores the urgent need for comprehensive studies in the capital of Iran. his analysis primarily focuses on the 2017 and 2020 seismic events and their causative faults. Additionally, we highlight the limitations of Tehran's seismic monitoring and active faults map by addressing examples of unidentified seismic unrest and faults. By tackling the significant challenges of seismic studies and evaluating the preparedness of people and cities for a major earthquake, we draw insights from recent earthquakes around Tehran. Results show that the Malard and Damavand earthquakes occurred on the previously unknown and Mosha faults, respectively. Sparse seismic stations limit route detection thresholds and location accuracy of seismicity near Tehran. In addition, we show that the dispersion of population and distressed fabrics in Tehran is clustered, and the vulnerability to earthquakes is linked to both physical and social factors. This study holds immense importance in enhancing seismological research and risk reduction strategies for the Tehran province.

Keywords: Earthquakes in Tehran, seismic monitoring, Mallard, Damavand, risk reduction, physical and social vulnerability

*Corresponding author: m.jamalreyhani@gmail.com

1 Introduction

Iran, intersected by several major faults, is one of the most seismically active countries globally. Throughout both historical and instrumental periods, it has experienced numerous destructive earthquakes including the 856 M_s 7.3 Damghan earthquake (Berberian and Yeats, 1999; Berberian and Yeats, 2016), the 1968 M_w 7.4 Dasht-e Bayaz earthquake (Berberian and Yeats, 1999), the 1990 M_w 7.3 Rudbar earthquake (Ajorlu et al., 2021), the 2003 M_w 6.6 Bam earthquake (Hesami et al., 2004), the 2012 Ahar-Varzeghan M_w 6.4 and 6.2 earthquake doublet (Ghods et al. 2015), and the 2017 M_w 7.3 Ezgeleh earthquake (Jamalreyhani et al., 2022).

The capital of Iran is located in the earthquake-prone Alborz mountain range (Figure 1). The deformation of the Alborz range is attributed to the northward shortening between the central Iranian block and the Eurasian plate. This deformation varies in style and intensity across and along the belt, causing the Central Alborz to exhibit the highest maximum shear strain rate (Khorrami et al., 2019). Since the early Pliocene, total shortening at the longitude of Tehran in central Alborz has been estimated at 30 km (Allen et al., 2003).

Seismicity and tectonic observations (Allen et al., 2003; Ritz et al., 2006) suggest that the overall oblique left-lateral motion across the Alborz is partitioned into separate strike-slip and thrust faults, both parallel to the trend of the belt. Within the Alborz, the Taleghan, Mosha, Firouzkuh, and Astaneh faults define a main left-lateral strike-slip corridor attesting to the partitioning of the deformation (Ritz et al., 2006; Shabanian and Hassanzadeh, 2022). In northern Alborz, the most important faults are the Khazar and the North Alborz reverse faults, which dip southward, whilst in the southern Alborz, the main active faults are the Mosha and North Tehran Faults (NTF), which dip northward (Figure 1). The Mosha fault and the Damavand stratovolcano are the two predominant features of the southern edge of the Central Alborz (Solaymani Azad et al. 2011).

The primary quaternary active fault zones in Tehran and its surroundings consist of the Mosha, NTF, Taleghan, Eshtehard, Kahrizak, Robat Karim, and Pishva faults, as illustrated in Figure 1 (Shabanian and Hassanzadeh, 2022). The Mosha fault is about 200 km long and modifies the drainage pattern of the region (Assereto, 1966). It has accommodated a total left-lateral displacement of 30–35 km, but its initiation time is not well constrained (Allen et al., 2003), and the present-day average rate is 3 mm/year (Trifonov et al., 1996; Ritz et al., 2006). On the other hand, the Mosha fault is one of the major active faults in Central Alborz due to its historical seismicity and its morphological signature (Pedrami, 1981; Bachmanov et al., 2004). This ~150 km long, ~N100E trending fault represents a potential seismic source threatening Tehran (Nazari et al., 2009).

During the 20th century, no strong seismic events were located in the southern part of the Central Alborz; however, several events of magnitudes larger than 5 were associated with the Mosha fault zone in the immediate vicinity northeast of Tehran (Berberian and Yeats, 1999). Most of focal mechanisms obtained from body wave modeling (Priestley et al., 1994; Jackson et al., 2002) or from the Global Centroid Moment Tensor (CMT) catalog (Ekström et al., 2012) indicate either reverse faulting or left-lateral strike-slip on faults parallel to the regional strike of the belt. Ashtari et al., (2005) demonstrated that left-lateral motion on both the Mosha and Garmsar faults.

The Mosha fault is crisscrossed by NTF at northern Tehran. This active and long fault zone (Solaymani Azad et al., 2011; Ghassemi et al., 2014; Tchalenko, 1975) indicates left-lateral strike-slip motion in the eastern (Solaymani Azad et al., 2011), middle (Abbassi and Farbod, 2009), and western (Trifonov et al., 1996) sections. Consequently, the Tehran megacity is a highly prone to large-magnitude earthquakes (Figure 1) (Berberian and Yeats, 2016; Kamranzad et al., 2020). This city serves as Iran's economic, administrative, political, and military hub while being situated in ahigh-seismicity zone (Berberian and Yeats, 1999; Berberian and Yeats, 2016). Tehran has experienced several devastating earthquakes in the past, including a ~M_w 7-7.4 earthquake in 1830 that resulted in thousands of deaths and injuries (Ambraseys and Melville, 2005; Berberian and Yeats, 2016).

Tehran's susceptibility to high seismic hazards, coupled with rapid urbanization, population growth, and various vulnerability factors, places it as a seismically vulnerable region (Hajibabaee et al., 2014; Berberian and Yeats, 2016). It ranks among the top 20 megacities worldwide facing a significant earthquake risk (Hajibabaee et al., 2014; Berberian and Yeats, 2016; Nazeri and Shomali, 2019; Kamranzad et al., 2020; JICA, 2000). Given the high seismic risk and vulnerability of Tehran, the government, residents, and, notably, the Earthquake science community must take proactive measures and precautions in preparation for potential seismic disasters.

The Earthquake science community plays a crucial role in providing essential insights and expertise to support earthquake preparedness and risk reduction efforts (Ben-Zion et al., 2022). Berberian and Yeats (2016) conducted the most comprehensive study by synthesizing all knowledge about regional earthquakes and faulting of the past in Tehran and its surroundings. However, in their research, no earthquakes with M > 5.0 have occurred within a radius of < 80 km around the center of Tehran. Since then, two 2017 and 2020 M_w ~5 earthquakes occurred in the vicinity of Tehran and caused several consequences.

In this study, we focus on the December 20, 2017, M_w 4.9 Malard and the May 7, 2020, M_w 5.0 Damavand seismic events and their causative faults (Figure 1). Additionally, we highlight the limitations

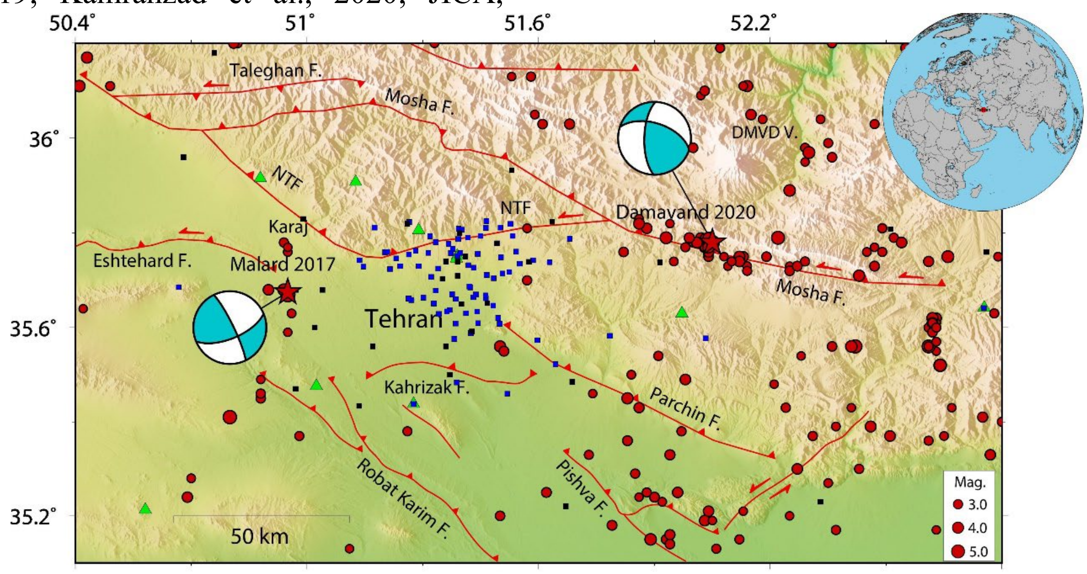

Figure 1. Tehran megacity and surrounding active faults. Red stars show the location of the 2017 Malard and 2020 Damavand earthquakes, and cyan beachballs are their focal mechanism solutions obtained in this study using waveform modeling. Red circles show the seismicity around Tehran from the IRSC catalog from 1996 to 2023. Green triangles show the seismic stations, and black and blue squares show the strong motion stations of the BHRC and TDMMO, respectively. NTH: North Tehran Fault, DMVD V.: Damavand Volcano. Red lines show the active faults (Hessami et al., 2003; Shabanian and Hassanzadeh, 2022).

of Tehran's seismic monitoring, barriers that affect scientific efforts, and "earthquake culture" (Mileti and Darlington, 1997) in Iran. We also evaluate Tehran's preparedness based on social and physical indices, especially urban distressed fabrics, to show the possible hotspots of damage. By addressing the significant challenges of seismic studies and evaluating the city's preparedness for a major earthquake, we draw valuable insights from those mentioned above, and the February 6, 2023, M_w 7.8 and 7.5 Kahramanmaraş doublet Turkey-Syria earthquakes, emphasizing the need for comprehensive studies in the capital of Iran.

2 The December 20, 2017, M_w 4.9 Malard Earthquake

The December 20, 2017, M_w 4.9 Malard earthquake occurred at ~11:30 p.m. local time (~8 p.m. UTC) near the town of Malard, approximately 40 kilometers west of Tehran (Figs. 1 and 2). The epicenter was close to Eshtehard and the NTF, east of the 1876 and northeast of the 1967 earthquakes (Berberian and Yeats, 2016). The earthquake caused significant damage to buildings and infrastructure in the affected area, including cracks in walls and ceilings, as well as power outages, resulting in reports of over 100 injuries.

According to the Iranian Seismological Center (IRSC: http://irsc.ut.ac.ir/) catalog, seismic unrest began in October 2017 and comprised dozens of small events of $M_n \sim 2–3$ south of Karaj city (Figure 2). Later, it culminated with M_w 4.9 Malard earthquakes, which was followed by several aftershocks (Niazpour and Shomali, 2023) (Figure 2). This pattern, reminiscent of precursory behavior observed in other regions (Bletery and Nocquet, 2023; Wetzler et al. 2023), which could be documented. However, due to limited seismic station coverage, the recorded data for this seismic activity is insufficient, and scientific questions remain unresolved.

Following the earthquake in the Malard, residents of Tehran and Karaj fled their homes, causing massive traffic jams as they sought safety from potential aftershocks or another large shock. According to local reports, 15 million liters of gasoline were consumed that night, causing more severe air pollution in Tehran after the earthquake. Some reports also indicated the disruption of the mobile phone network in several areas due to overuse. Since the Malard earthquakes, due to the lack of data, no detailed scientific study has been conducted on this seismic event, leaving the mechanism and causative fault ambiguous. We use waveform records from a few seismic stations (Figure 1) to obtain the focal mechanism of this event.

We apply the probabilistic earthquake source inversion framework for the point source modeling of the Malard earthquake (Heimann et al. 2018; Jamalreyhani et al. 2022). To solve the nonlinear optimization problem efficiently, we use Bayesian bootstrap optimization (BABO, as implemented in the inversion framework Grond by Heimann et al., 2018). This method starts exploring model space by taking samples from a uniform distribution within given parameter bounds and has been successfully applied to other earthquakes in Iran (e.g., Jamalreyhani et al. 2021, Hassanzadeh et al., 2024).

We conducted the Moment Tensor (MT) inversion to fit three-component full displacement waveforms in the frequency band of 0.025–0.09 Hz in both time and frequency domains. Synthetic seismograms were computed using precalculated Green's functions (Heimann et al., 2019) based on a modified velocity model from the studies of Soltani-Moghadam et al. (2019) and Shirzad et al. (2019). Figure 2 illustrates the focal mechanism result of the Malard event and waveform fits. Except for the dip, the resolved focal mechanisms align with the

Global CMT solution (Strike1, Dip1, Rake1 of 71°, 80°, 24°, and Strike2, Dip2, Rake2 of 336°, 66°, 169°). The focal mechanism results using the waveform modeling show the strike-slip mechanisms, either a right-lateral slip striking NWSE or a left-lateral slip striking NESW. Naserieh et al. (2023), based on directivity analysis, suggested the left-lateral movement for the Malard earthquake. However, suspicions arise regarding the presence of a right-lateral ~NS striking fault when considering the seismic activity in October on the same fault plane as the Malard sequence (Figure 1). We also determined a centroid depth of 11±2 km (Figure 2) and a moment magnitude of M_w 4.8±0.1. The uncertainties are estimated based on the bootstrap model ensembles and are given as 68% confidence intervals (Figure 2). It is demonstrated that the north Eshtehard fault may extend as a basement fault to a depth of approximately 18 km (Movaghari and Javan, 2018).

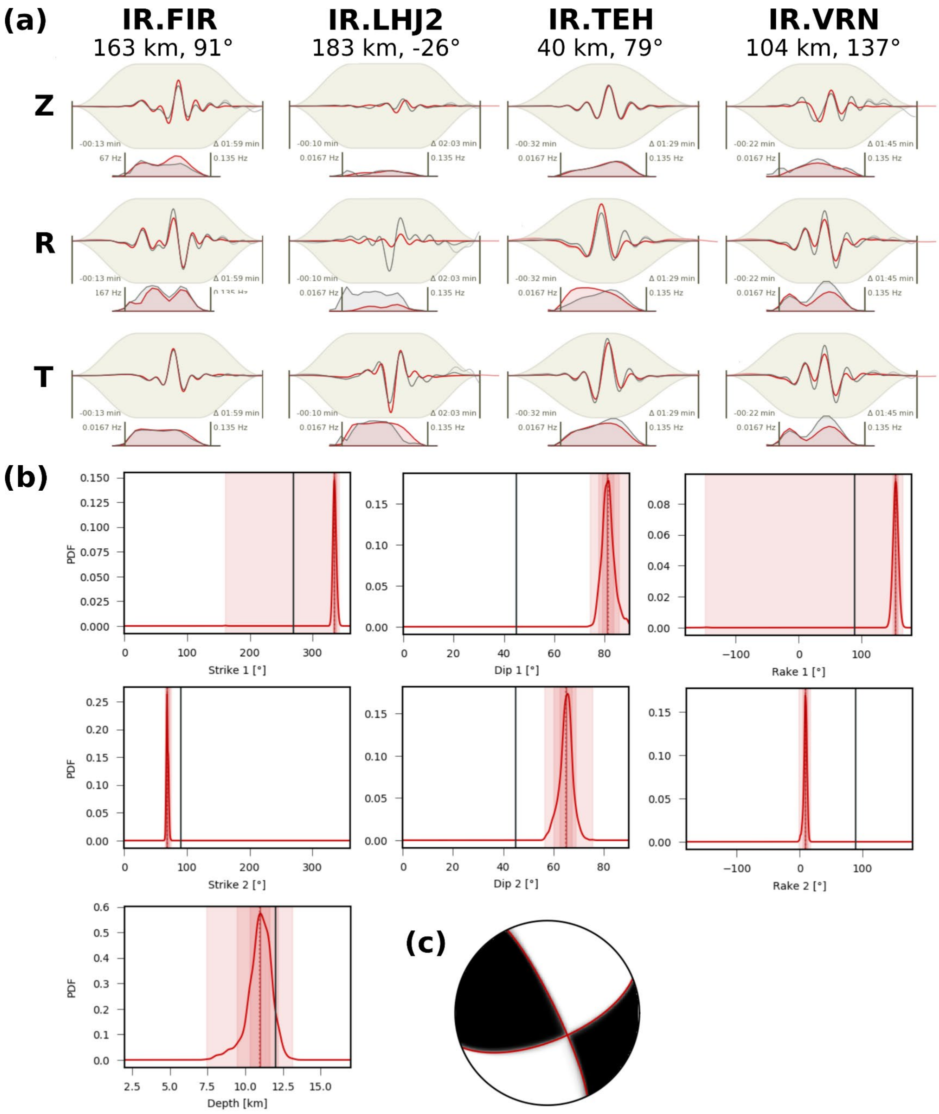

Figure 2. a) Waveform fits of December 20, 2017, M_w 4.9 Malard earthquake in time and frequency domains. Red and gray waveforms show synthetic and observed records, respectively. Information on the top of the waveform gives station names with transverse (T), radial (R), or vertical (Z) components, as well as station distance and azimuth. b) The probability distribution function of strikes, dips, rakes, and depth is also shown. The solid red vertical line gives the median of the distribution, and the dashed red vertical line gives the mean value. The overlapping red-shaded areas show the 68% confidence intervals (innermost area), the 90% confidence intervals (middle area), and the minimum and maximum values (widest area). c) The fuzzy full MT solution.

3 The May 7, 2020, M_w 5.0 Damavand Earthquake

On May 7, 2020, an M_w 5.0 earthquake struck the Damavand region of Tehran province in Iran. The earthquake occurred at a depth of 13 km and was felt in several nearby cities (Baftipour et al., 2022; Azghandi et al., 2023). While there were no immediate reports of casualties or significant damage, some buildings in the affected areas suffered cracks and damage (Zare, 2020). The earthquake also caused panic among residents, with 2 casualties, who rushed out of their homes and into the streets. The Damavand region is located near several active fault lines and has experienced several earthquakes in the past. The largest and most destructive earthquakes in the vicinity of the hypocenter of the Damavand earthquake were the 1996 M_w 6.5 and 1830 M_w 7.1 earthquakes (Berberian and Yeats, 2016). The preliminary source mechanism of the Damavand earthquake indicates the strike-slip mechanism, with either a left-lateral slip on a near-vertical plane striking EW or a right-lateral slip on a near-vertical plane striking NS (Global CMT; Baftipour et al., 2022). Due to the relatively weak magnitude and deeper centroid depth of ~13 km (figs. S1), which aligns with the Mosha fault locking depth (Vajedian et al. 2015), no static surface displacement was reported in the coseismic interferograms (Büyükakpınar et al., 2021). The mainshock was preceded by a foreshock with M_n 2.9 and followed by a significant aftershock sequence, including ten events with M_n 3+.

The Damavand earthquake was recorded by digital accelerometers from the strong-motion network in Iran (Figure 3), which belongs to the Building and Housing Research Center (BHRC). The closest station (MOA3), with an epicentral distance of 13 km, recorded the second-largest peak ground acceleration (PGA) of 1.12 m s^{-2}. The largest recorded PGA at the station RDH1, with a 22 km epicentral distance, is about 1.21 m s^{-2} in Rudhen (Momeni and Madariaga, 2022). We evaluate the seismic sequence of the Damavand earthquake and obtain the MT inversion for this event and its larger aftershocks (Figure 3). We applied the probabilistic earthquake source inversion framework using broadband seismograms (Figs. 3; S1). We set up the MT inversion for the Damavand mainshock to fit three-component full displacement waveforms in the frequency band of 0.025–0.09 Hz in time and frequency domains (Figure S1).

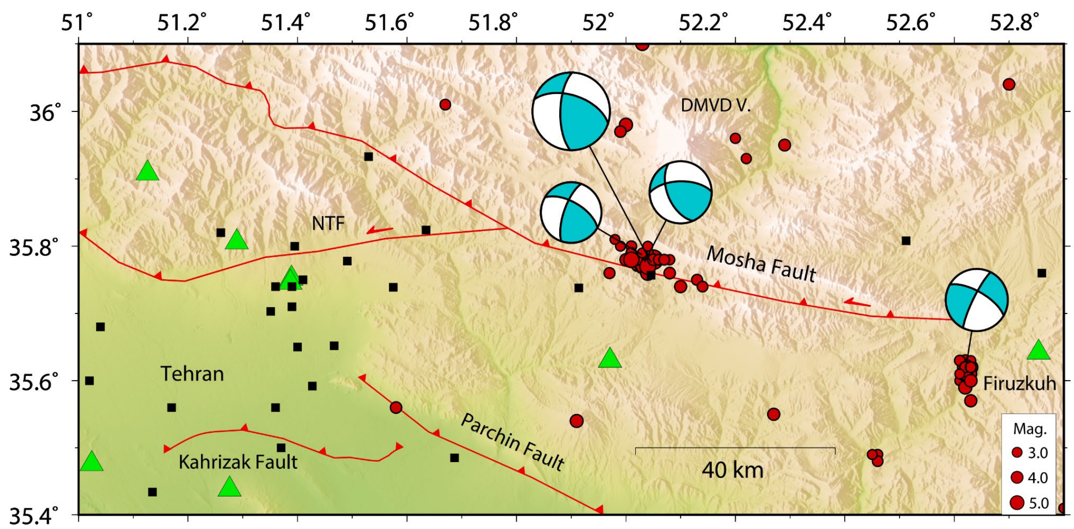

Figure 3. Focal mechanism of the May 7, 2020, an M_w 5.0 Damavand earthquake and its larger aftershocks, and the July 12, 2020 M_w 4 Firuzkuh earthquake. Red circles are earthquakes with magnitudes larger than 3 around Tehran during 2020-2023, from the IRSC catalog. Green triangles show the seismic station and black squares represent the strong-motion stations. Red lines are active faults. DMVD V: Damavand volcano.

The focal mechanism results show that the causative fault plane for the Damavand mainshock has a strike of 178°±10°, assuming NW-SE fault orientation, based on the Mosha fault trace, and a dip of 60°±2°, a left-lateral strike-slip with reverse motion mechanism given a rake of 140°±10° (Figure 3). Two largest aftershocks have almost similar mechanisms with the Damavand mainshock and confirm that they occurred at the same fault plane (Figure 3).

Our MT inversion for the mainshock is in general agreement with the results of (Momeni and Madariaga, 2022). They also modeled the finite fault that suggests the mainshock rupture propagated towards the northwest. This directivity enhanced the peak acceleration in the direction of rupture propagation, observed in the strong-motion records. The azimuthal pattern of the PGA (higher PGA for stations in front of the rupture) supports the westward direction. This explains why people in Tehran and Karaj cities strongly felt this earthquake (Momeni and Madariaga, 2022; Azghandi et al., 2023). For instance, the FHS2 station, with a 53 km epicentral distance, in front of the rupture recorded the PGA of 0.85 m s^{-2} but the ARJ1 station, with a 37 km epicentral distance, in the opposite direction, recorded the PGA of 0.13 m s^{-2}.

Later after the Damavand earthquake, on July 12, 2020, another seismic unrest was recorded ~60 km southeast of the Damavand earthquake, close to Firuzkuh (Figure 3), where we conducted the mechanism of a larger event (2020-07-12T07:19:55 M 4) at a depth of 3 km (Figure S2). We set up the MT inversion for this event to fit three-component displacement waveforms in five stations in the frequency band of 0.02–0.08 Hz (Figure S2). Results show the shallow strike-slip motion (Figure 3). Yet, the specific fault responsible for this cluster remains unidentified, and there have been no reports of an active fault in this region.

4 Limitations of Tehran's seismic monitoring, faults map, and seismological data

Established in 1957, the Institute of Geophysics, University of Tehran (IGUT), is a leading scientific center, operating Iran's largest seismic network, which includes 126 stations, with short periods and broad bands sensors (Hosseini et al. 2019). These stations are overseen by the IRSC. A noteworthy development since 2015 is the data-sharing collaboration between IRSC and the International Institute of Earthquake Engineering (IIEES), which has led to improved seismic station azimuthal coverage and relatively reduced location errors (Figure 1). The IIEES has played a crucial role in earthquake reporting and monitoring in Iran since 1998 (Hosseini et al. 2019). The IRSC waveforms are available for events with a magnitude larger than M_n 4 in Nanometrics (Y-file) format, and the IRSC catalog is available for M_n 2.5+. In addition, waveforms of IIEES are available for events with a magnitude larger than M_l 4.5 in the SEISAN binary format.

Furthermore, two strong motion networks are also operated in Iran (Figure 1). The Iranian Strong Motion Network (ISMN) was established in 1973 and overseen by the BHRC (Farajpour et al., 2018). The ISMN operates a network of over 2000 strong motion stations strategically positioned across the country. In addition to ISMN, the Tehran Disaster Mitigation and Management Organization (TDMMO) recently operated a local network in Tehran for the development of the early warning system (Figure 1).

Seismic coverage in Iran is confined to sparse stations, limiting route detection thresholds and location accuracies (Karasözen et al., 2019) and also preventing focal mechanisms (Hosseini et al., 2019) from being determined for most small-to-moderate earthquakes (e.g., fore- and aftershocks of the Malard earthquake). The sparse seismic network and rapid urban development in Tehran and the surrounding area, in combination with the proximity of earthquake faulting, challenge an accurate resolution of the active faults network geometry (Shabanian and Hassanzadeh, 2022).

The lack of sufficient seismic stations in Tehran poses a significant challenge for the earth science community. Without an adequate network of monitoring stations, it becomes challenging to accurately detect and record small earthquakes that might be occurring in the region. Small earthquakes, though less destructive than larger ones, are essential for monitoring as they provide valuable information about the underlying fault systems and seismic activity in the region (e.g., Wang et al., 2014; Ide, 2019). They can serve as indicators of potential larger seismic events, and studying them is crucial for understanding the overall seismic hazard and risk associated with Tehran. A comprehensive earthquake catalog obtained from microseismic studies helps researchers understand the development of mapped surface faults at depth and their movement, earthquake recurrence, and other geophysical processes (Ross et al., 2019).

5 How do physical and social factors affect Tehran?

Implementing urban planning principles and enhancing the physical infrastructure of a city could contribute to risk reduction in areas prone to earthquakes (Ciborowski, 1982). In this regard, Oki and Osaragi (2017) assessed the effects of physical indices such as installing fire extinguishers, seismo-sensitive breakers, street accessibility, and roadside buildings in Japan. They discovered that applying physical systems reduces damage significantly (Oki & Osaragi, 2017). Also, Amini et al (2010), and Yaghoob Nejad Asl (2018) found that the safety and security of urban land use or physical aspects of the city is the most important indicator toward planning for leveling off natural hazards' damages. Furthermore, they pointed out that spatial dispersion of urban land use, population density, building density, and size of buildings are crucial for assessing the vulnerability of urban texture toward earthquakes. Rashed and Weeks (2003) have used physical indicators such as the function of bridges, medical emergency services, hospitals, highways, and the cost of building recovery to determine a city's vulnerability to earthquakes (Rashed and Weeks, 2003).

There are several methods to assess a city’s preparedness for natural hazards like earthquakes. Physical, social, economic, managerial, and political aspects are useful indices, all contributing to the preparedness of society. Here, we assess Tehran's preparedness based on social and physical indices, especially urban distressed fabrics, to show the possible hotspots of damage.

Statistics show that Tehran, with 22 municipal districts, has about 9430625 people (Tehran Statistical Center: https://www.amar.org.ir/english). Spatial dispersion of population reveals that districts 4, 5, 2, 15, 1, 14, and 8, respectively, with about 4.96 million people accounted for the largest (46%) populated regions. Also, an assessment of the density indicator shows that the average density is 153 people per Hectare, which means a high level of concentration in Tehran accompanied by population dispersion across the districts. The highest rate of density belongs to districts 10, 17, and 8, with 424, 396, and 375 respectively. In contrast, districts 22, 21, and 9, with 40, 41, and 100 people density per Hectare, are the districts with low rates of concentration. Therefore, it is clear that Tehran's population is primarily concentrated in the interior districts close to the city center.

We employed Moran's spatial autocorrelation index to assess the spatial pattern of the population in Tehran. Based on

Moran's principles, autocorrelation emerges when there is a connection between values of a variable situated in close geographical proximity. In cases where variable values are distributed randomly, no correlation should exist among them (Kumari et al., 2019). Moran's autocorrelation index in Tehran, with an index of 0.26 and a z-score of 1.91, reveals that the population distribution in Tehran is highly clustered (Figure 4).

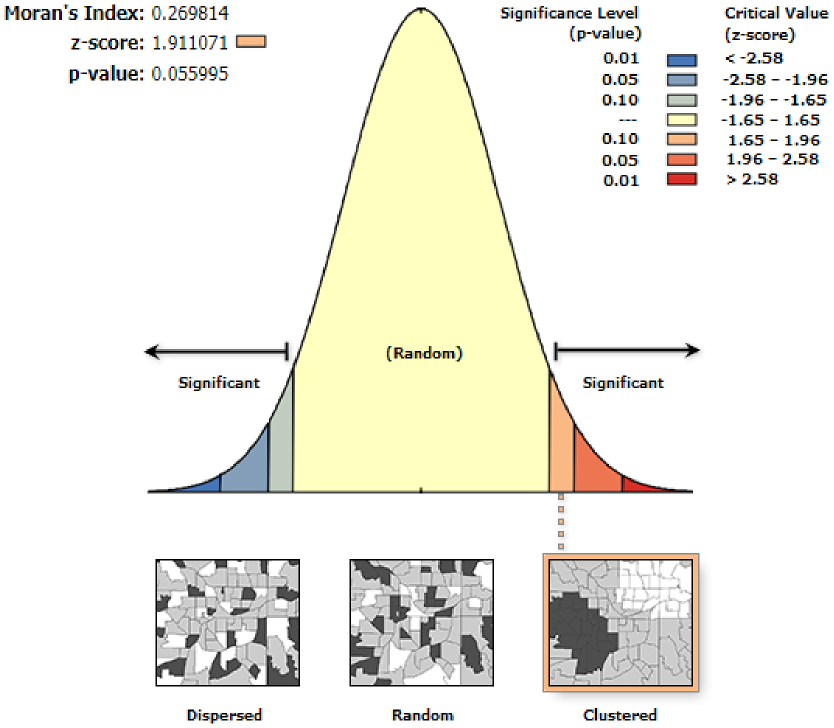

Figure 4. The pattern of population distribution in Tehran based on Moran's index.

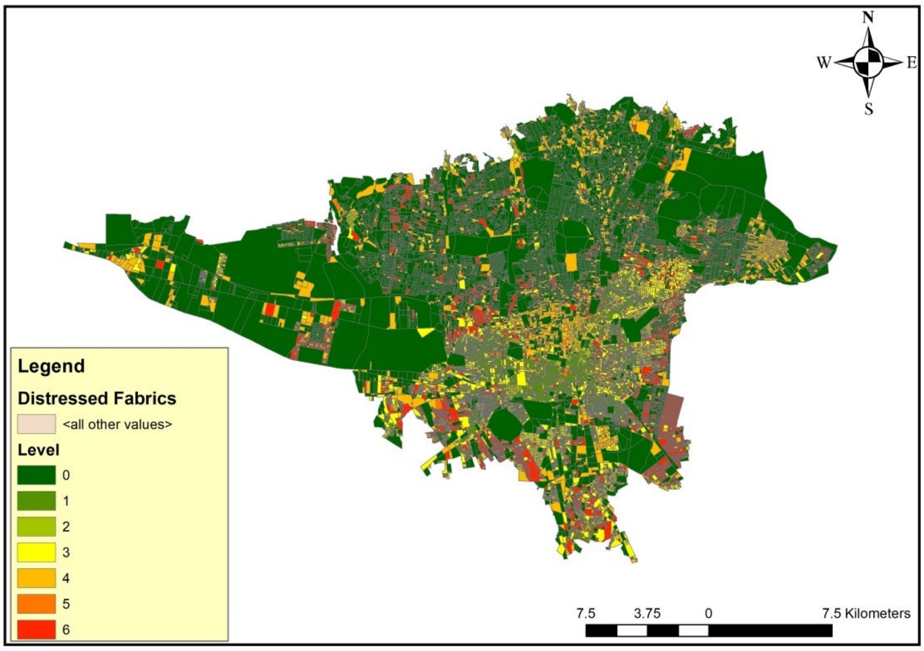

Figure 5. Spatial dispersion of urban distressed fabrics in Tehran.

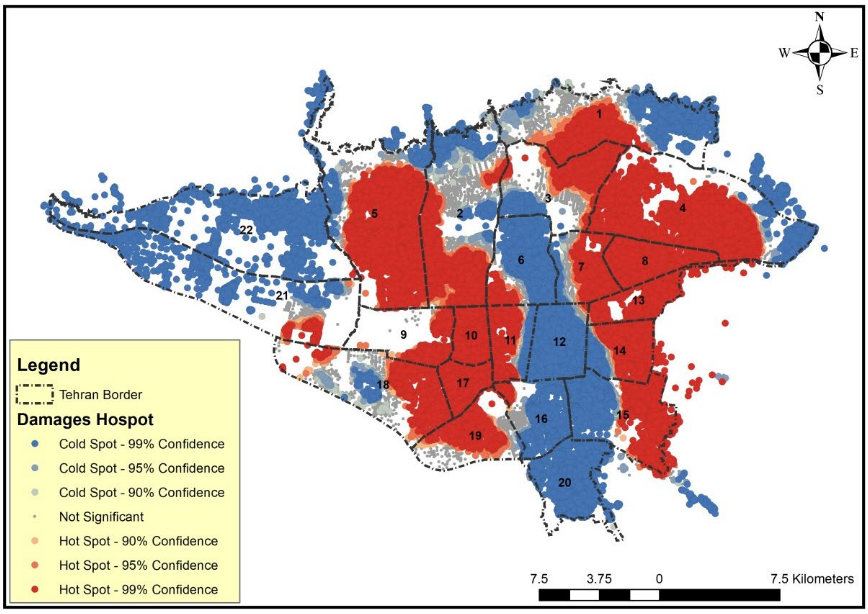

Figure 6. Tehran's hotspot of damages during the earthquake.

The second factor impacting Tehran during an earthquake is the presence of urban distressed fabrics, which, based on the latest consensus, encompass about 3271 Hectares, which represents ~37% of Tehran's population (Figure 5). Turning to the spatial dispersion of unsustainability in the buildings reveals that districts 4, 5, 6, 21, and 22 have the least amount of distressed fabrics in Tehran, while, districts 12, 10, and 11 accounted for the highest part of urban distressed fabrics with 563, 428, and 355 Hectares respectively.

Overlaying the layers of population, urban distressed fabrics, and density data yield a map of hotspots for damages in Tehran after the earthquake. The damaged hotspot is divided into a cold and hot spot. Hotspots are regions where the rate of damage is high due to the high concentration of population and urban distressed fabrics. Districts 8, 10, 13, and 17 are completely hot spots, while districts 1, 2, 3, 4, 5, 6, 7, 9, 11, 14, 15, 16, 18, 19, and 21 are partially hot or cold spots. In addition, districts 20, 12, and 22 are completely located within the cold spots. These results correlated with the risk map of the multi-geo-hazards in Tehran (Zare, 2020) and the higher value of annualized earthquake loss suggested by Kalantari et al. (2023).

6 Discussion and Conclusion

Earthquakes in Tehran area are foreseeable and inevitable. Recent years have seen growing concern about the potential impact of an earthquake on Tehran, particularly given its high population density and inadequate infrastructure to withstand seismic activity (Berberian and Yeats, 2016, and references therein). Recent two moderate magnitude earthquakes around Tehran (The 20 December 2017 M_w 4.9 Malard and the 7 May 2020 M_w 5.0 Damavand earthquakes) highlight the necessity of detailed studies in the Tehran metropolis. Results show that the Malard and Damavand earthquakes occurred on the previously unknown and Mosha faults, respectively. The casualties and social consequences following these earthquakes indicate vulnerability and inadequate earthquake culture (Mileti and Darlington, 1997; Karasözen et al., 2023) regarding disaster preparedness. A probabilistic seismic risk assessment quantified Tehran's annualized earthquake loss as \$1.05 billion (Kalantari et al., 2023).

Jaiswal and Wald (2010) highlighted fatality rates in different countries, and due to the building construction and quality, Iran is 1,000 times more vulnerable to earthquakes than California, where the annualized direct economic losses from earthquakes are estimated to be around $4 billion (Ben-Zion et al., 2022), having an area approximately 420 times larger than Tehran.

On February 6, 2023, two destructive M_w 7.8 and 7.5 earthquakes at a shallow depth of ~7 km struck south Turkey and northern Syria (Barbot et al., 2023). These earthquakes resulted in over 50,000 casualties and 100,000 injured people. The first M_w 7.8 mainshock occurred at 01:17 AM UTC, and the epicenter is located at a splay fault, 20 km near the East Anatolian Fault (Dal Zilio and Ampuero, 2023). The second M_w 7.5 earthquake occurred 9 hours later ~100 km north of the first shock on the east-west trending left lateral Sürgü-Cardak Fault. These earthquakes highlighted the need to strictly apply building codes in Turkey (Karasözen et al., 2023). This disaster is a significant lesson that should be considered for other megacities, such as Tehran, to mitigate the impact of future earthquakes, such as strengthening building codes, retrofitting old buildings, and having emergency and disaster plans. Moreover, these seismic events underscore the likelihood of multiple earthquakes (e.g. earthquake doublet) in Tehran, given its location intersected by several crisscrossed active faults.

From the Malard earthquake experience in 2017, a comprehensive emergency response plan that includes evacuation routes, emergency shelters, and supplies is essential. In addition, early warning systems can provide crucial time for people to evacuate and take necessary precautions before the earthquake strikes (Enferadi et al., 2021). Furthermore, educating the public on earthquake safety measures can help minimize damage and loss of life (Mileti et al., 2002; Karasözen et al., 2023; Hetényi and Subedi, 2023). Iran should invest in public education campaigns that teach residents how to prepare for earthquakes, what to do during and after an earthquake, and reduce the gap (Toomey, 2016) between scientific knowledge and action.

Collaborative efforts between the Earthquake Science community, government agencies, and other stakeholders are essential to bolster a city's resilience and safeguard its population against earthquakes (Ben-Zion et al., 2022). The scientific community needs to garner decision-makers' attention and secure funding resources to advance research, seismic monitoring, and the development of innovative technologies for possible earthquake prediction and risk mitigation. Open scientific discussion and data can promote and enhance many key aspects of modern science (Karasözen et al., 2023; Dallo et al., 2023). The Global Earthquake Science community should intensify its efforts to collaborate with Iran's local, state, and national government agencies. By joining forces, they can develop a groundbreaking infrastructure dedicated to earthquake research (Ben-Zion et al., 2022). This endeavor aims to achieve a scale and magnitude comparable to the achievements of select scientific communities that have successfully undertaken similar initiatives. Furthermore, monitoring seismic activity to detect changes that could indicate an impending earthquake (e.g., a pre-course signal before large earthquakes) requires a vast network of sensors. Moreover, sophisticated new data analysis tools (e.g., Machine learning techniques, see Mousavi and Beroza, 2023) gain insights into earthquake processes and yield to significantly improve the mitigation of seismic risks.

Although short-term prediction of the magnitude, time, and location of earthquakes is currently not possible, behavior that is considered precursory has been documented (Bletery and Nocquet, 2023; Wetzler et al., 2023). The high-rate GPS time series analysis indicates large earthquakes often begin with a precursory slip phase before the rupture (Bletery and Nocquet, 2023). For instance, using dense GPS data along this fault, Aktug et al. (2016) show two seismic gaps that can produce earthquakes M > 7 along the East Anatolian Fault System. Furthermore, with the availability of close observations along the North Anatolian Fault, Bouchon et al. (2011) could detect that the 1999 Izmit earthquake was preceded for 44 minutes by a phase of slow slip based on evidence of a succession of repetitive seismic bursts, accelerating with time and increasing low-frequency seismic noise.

With more comprehensive and effective earthquake monitoring, it may be possible to recognize a preparation phase before a significant earthquake in Tehran. In addition, due to the rapid urban growth in Tehran, geology and remote sensing do not significantly contribute to the identification of faults. Therefore, seismology plays a role but requires the dense seismic network to record small earthquakes and reveal the geometry and mechanisms of faults. Consequently, our knowledge about Tehran's faults is limited, such as the December 20, 2017, Malard and July 12, 2020 Firuzkuh earthquake sequence (Figs. 2, and 3) in which the specific fault responsible for these clusters was unidentified.

Tehran's vulnerability to earthquakes is intricately linked to physical and social factors. The concentration of the population in specific regions, as revealed by spatial analysis, coupled with the prevalence of urban distressed fabrics, accentuates the potential impact of seismic events. Identifying hotspots, such as regions 8, 10, 13, and 17, underscores the urgency for targeted interventions and preparedness measures in these areas. Integrating findings from various studies, ranging from urban planning principles to density assessments, provides a holistic understanding of the challenges Tehran faces in mitigating earthquake risks. As urban areas continue to expand and face the increasing threat of natural disasters, the insights gained from this study can inform policymakers and urban planners in developing more resilient strategies to safeguard Tehran's physical and social fabric.

Acknowledgments
We thank Iranian Seismological Center (IRSC), International Institute of Earthquake Engineering (IIEES), and the Iranian Strong Motion Network (ISMN) for providing data. We express our gratitude to the editor and reviewers for their valuable comments.

Data and Resources
Some of the maps were prepared using the Pyrocko toolbox (Heimann et al., 2017; https://pyrocko.org/) and GMT 5 software (Wessel et al., 2013; https://www.generic-mapping-tools.org/). The probabilistic source inversion was performed with the Grond framework (Heimann et al., 2018; https://pyrocko.org/grond/docs/current/).

Competing Interests
The authors have no relevant financial or non-financial interests to disclose.

References
Abbassi M, Farbod Y (2009). Faulting and folding in quaternary deposits of Tehran’s piedmont (Iran). *Journal of Asian Earth Sciences, 34*(4), 522-531. https://doi.org/10.1016/j.jseaes.2008.08.001.

Ajorlou N, Hollingsworth J, Mousavi Z, Ghods A, Masoumi Z (2021). Characterizing near-field surface deformation in the 1990 Rudbar earthquake (Iran) using optical image correlation. *Geo-*

chemistry, Geophysics, Geosystems, 22(6), e2021GC009704. https://doi.org/10.1029/2021GC009704.

Aktuğ B, Özener H, Doğru A, Sabuncu A, Turgut B, Halıcıoğlu K. and Yılmaz O (2016). Slip rates and seismic potential on the East Anatolian Fault System using an improved GPS velocity field. *Journal of Geodynamics*, 94–95, 1–12, https://doi.org/10.1016/j.jog.2016.01.001.

Allen M, Ghassemi M, Shahrabi M, Qorashi M (2003). Accommodation of late Cenozoic oblique shortening in the Alborz range, northern Iran. *Journal of Structural Geology, 25*(5), 659-672. https://doi.org/10.1016/S0191-8141(02)00064-0.

Ambraseys N. N, Melville C. P (2005). *A history of Persian earthquakes*: Cambridge university press. https://doi.org/10.1002/eqe.4290110412.

Amini E, Habib F, Mojtahedzadeh G. H (2010). Land Use Planning and its effects on reduced city vulnerability Against Earthquake. *Journal of Environmental Science and Technology, 12*(3), 161-174.

Ashtari M, Hatzfeld D, Kamalian N (2005). Microseismicity in the region of Tehran. *Tectonophysics, 395*(3-4), 193-208. https://doi.org/10.1016/j.tecto.2004.09.011.

Assereto R (1966). *Geological Map of Upper Djadjerud and Lar Valleys Central Elburz, Iran*.

Azad S. S, Ritz J.-F, Abbassi M. R (2011). Left-lateral active deformation along the Mosha–North Tehran fault system (Iran): Morphotectonics and paleoseismological investigations. *Tectonophysics, 497*(1-4), 1-14. https://doi.org/10.1016/j.tecto.2010.09.013.

Azghandi, M., Abbassi, M.R., Javan Doloei, G., Sadidkhouy, A. (2023). Fault-kinematic and stress state investigation using focal mechanism solution along the Mosha fault, Alborz Mountain: implication for changing stress tectonic regime. Iranian Journal of Geophysics, 16(4), 165-174. DOI: https://dorl.net/dor/20.1001.1.20080336.1401.16.4.12.5

Bachmanov D, Trifonov V, Hessami K. T, Kozhurin A, Ivanova T, Rogozhin E, Jamali F (2004). Active faults in the Zagros and central Iran. *Tectonophysics, 380*(3-4), 221-241. https://doi.org/10.1016/j.tecto.2003.09.02.

Baftipour M, Jarahi H, Polat G, Seifilaleh S (2022). Damavand Earthquake of 2020 the Mainshock or an Alarm for Disaster for the Capital of Iran. AJEAS 15, 51–58. https://doi.org/10.3844/ajeassp.2022.51.58.

Barbot S, Luo H, Wang T, Hamiel Y, Piatibratova O, Muhammad T, Gurbuz G (2023). Slip distribution of the February 6, 2023 Mw 7.8 and Mw 7.6, Kahramanmaraş, Turkey earthquake sequence in the East Anatolian fault zone. *Seismica, 3*(2). https://doi.org/10.26443/seismica.v2i3.502.

Ben-Zion Y, Beroza G. C, Bohnhoff M, Gabriel A. A, Mai P. M (2022). A grand challenge international infrastructure for earthquake science. Seismological Research Letters, 93 (6): 2967–2968.. https://doi.org/10.1785/0220220266.

Berberian M, Yeats R. S (1999). Patterns of historical earthquake rupture in the Iranian Plateau. *Bulletin of the Seismological Society of America, 89*(1), 120-139. https://doi.org/10.1785/BSSA0890010120.

Berberian M , Yeats R.S (2016). Tehran: An earthquake time bomb. , in Sorkhabi, R, ed, Tectonic Evolution, Collision, and Seismicity of Southwest Asia: In Honor of Manuel Berberian's Forty-Five Years of Research Contributions: Geological Society of America Special Paper 525, p. 87–170. https://doi.org/10.1130/2016.2525(04).

Bletery Q, Nocquet J.-M (2023). The precursory phase of large earthquakes. *Science, 381*(6655), 297-301. https://doi.org/10.1126/science.adg2565.

Bouchon M, Karabulut H, Aktar M, et al., 2011. Extended nucleation of the 1999 Mw 7.6 Izmit earthquake. *Science* 331, 877-880. DOI: 10.1126/science.119734.

Büyükakpınar P, Jamalreyhani M, Rezapour M, et al (2021). *Rupture process of the 7 May 2020 Mw 5.0 Tehran earthquake and its relation with the Damavand stratovolcano, and Mosha Fault.* Paper presented at the EGU General Assembly Conference Abstracts. https://doi.org/10.5194/egusphere-egu21-1759.

Ciborowski A (1982). Physical development planning and urban design in earthquake-prone areas. *Engineering Structures, 4*(3), 153-160. https://doi.org/10.1016/0141-0296(82)90003-7.

Dal Zilio L, Ampuero J. Earthquake doublet in Turkey and Syria. Commun Earth Environ. 2023; 4: 71. In. https://doi.org/10.1038/s43247-023-00747-z.

Dallo I, Herrmann M, Supino M, Bayona J. A, Khawaja A. M, Scaini C (2023). The need for open, transdisciplinary, and ethical science in seismology. *Seismica, 2*(2). https://doi.org/10.26443/seismica.v2i2.470.

Enferadi S, Shomali Z. H, Niksejel A (2021). Feasibility study of earthquake early warning in Tehran, Iran. *Journal of Seismology, 25*(4), 1127-1140. https://doi.org/10.1007/s10950-021-10014-3.

Farajpour Z, Zare M, Pezeshk S, Ansari A, Farzanegan E (2018). Near-source strong motion database catalog for Iran. *Arabian Journal of Geosciences, 11*, 1-16. https://doi.org/10.1007/s12517-018-3413-x.

Ghassemi M. R, Fattahi M, Landgraf A, Ahmadi M, Ballato P, Tabatabaei S. H (2014). Kinematic links between the eastern Mosha fault and the North Tehran fault, Alborz range, northern Iran. *Tectonophysics, 622*, 81-95. https://doi.org/10.1016/j.tecto.2014.03.007.

Hajibabaee M, Amini-Hosseini K, Ghayamghamian M (2014). Earthquake risk assessment in urban fabrics based on physical, socioeconomic and response capacity parameters (a case study: Tehran city). *Natural hazards, 74*, 2229-2250. https://doi.org/10.1007/s11069-014-1300-7.

Heimann S, Isken M, Kühn D et al (2018). Grond: A probabilistic earthquake source inversion framework. https://doi.org/10.5880/GFZ.2.1.2018.003.

Heimann S, Kriegerowski M, Isken M et al (2017). Pyrocko-An open-source seismology toolbox and library. https://doi.org/10.5880/GFZ.2.1.2017.001.

Heimann S, Vasyura-Bathke H, Sudhaus H, Isken M. P, Kriegerowski M, Steinberg A, Dahm T (2019). A Python framework for efficient use of pre-computed Green's functions in seismological and other physical forward and inverse source problems. *Solid Earth, 10*(6), 1921-1935. https://doi.org/10.5194/se-10-1921-2019.

Hassanzadeh, M. A., Jamalreyhani, M., Arvin, S., & VahidRavesh, S. (2024). The link between gas extraction and shallow seismicity around the Dalan gas field of Zagros Mountains, Iran. Physics of the *Earth and Planetary Interiors,* 355, 107246. https://doi.org/10.1016/j.pepi.2024.107246

Hessami K, Jamali F, Tabassi H, (2003). Major Active Faults of Iran, Map, International Institute of Earthquake Engineering and Seismology (IIEES), Tehran, Iran, scale 1:2,500,000.

Hessami K. Tabassi H. Abbassi M.R. Azuma T. Okumura K. Echigo T. Kondo H., 2004. Surface expression of the Bam Fault Zone in Southeastern Iran: Causative Fault of the 26 December 2003 Bam Earthquake, Journal of Seismology and Earthquake Engineering, 4, 5–14.

Hetényi G, Subedi S (2023). A Call to Action for a Comprehensive Earthquake Education Policy in Nepal. *Seismica,* *2*(2). https://doi.org/10.26443/seismica.v2i2.242.

Hosseini H, Pakzad M, Naserieh S (2019). Iranian regional centroid moment tensor catalog: Solutions for 2012–2017. *Physics of the Earth and Planetary Interiors, 286*, 29-41. https://doi.org/10.1016/j.pepi.2018.11.001.

Ide, S. (2019). Frequent observations of identical onsets of large and small earthquakes. *Nature* 573, 112–116. https://doi.org/10.1038/s41586-019-1508-5

Jackson J, Priestley K, Allen M,Berberian M (2002). Active tectonics of the south Caspian basin. *Geophysical Journal International, 148*(2), 214-245. https://doi.org/10.1046/j.1365-246X.2002.01588.x.

Jaiswal K, Wald D (2010). An empirical model for global earthquake fatality estimation. *Earthquake Spectra, 26*(4), 1017-1037. https://doi.org/10.1193/1.3480331.

Jamalreyhani M, Pousse-Beltran L, Büyükakpınar P et al (2021). The 2019–2020 Khalili (Iran) Earthquake Sequence—Anthropogenic Seismicity in the Zagros Simply Folded Belt? *Journal of Geophysical Research: Solid Earth, 126*(12), e2021JB022797. https://doi.org/10.1029/2021JB022797.

Jamalreyhani M, Rezapour M, Cesca S, Dahm T, Heimann S, Sudhaus H, Isken M. P (2022). Insight into the 2017–2019 Lurestan arc seismic sequence (Zagros, Iran); complex earthquake interaction in the basement and sediments. *Geophysical Journal International, 230*(1), 114-130. https://doi.org/10.1093/gji/ggac057.

JICA, C (2000). The study on seismic microzoning of the Greater Tehran Area in the Islamic Republic of Iran. *Pacific Consultants International Report, OYO Cooperation, Japan*, 291-390.

Kalantari M, Firuzi E, Ahmadipour M, Sorooshian S (2023). Estimating annualized earthquake loss for residential buildings in Tehran, Iran. *Bulletin of Earthquake Engineering, 21*(4), 2259-2280. https://doi.org/10.1007/s10518-022-01604-8.

Kamranzad F, Memarian H, Zare M (2020). Earthquake risk assessment for Tehran, Iran. *ISPRS International Journal of Geo-Information, 9*(7), 430. https://doi.org/10.3390/ijgi9070430.

Karasözen E, Buyukakpinar P, Ertuncay D, Havazlı E, Oral E (2023). A call from early-career Turkish scientists: seismic resilience is only feasible with "earthquake culture". *Seismica, 2*(3). https://doi.org/10.26443/seismica.v2i3.1012.

Karasözen E., Nissen E., Bergman E.A., Ghods A (2019). Seismotectonics of the Zagros (Iran) From Orogen-Wide, Calibrated Earthquake Relocations. Journal of Geophysical Research: Solid Earth 124, 9109–9129.

https://doi.org/10.1029/2019JB017336.

Khorrami F, Vernant P, Masson F, Nilfouroushan F et al (2019). An up-to-date crustal deformation map of Iran using integrated campaign-mode and permanent GPS velocities. *Geophysical Journal International, 217*(2), 832-843. https://doi.org/10.1093/gji/ggz045.

Kumari M, Sarma K, Sharma R (2019). Using Moran's I and GIS to study the spatial pattern of land surface temperature in relation to land use/cover around a thermal power plant in Singrauli district, Madhya Pradesh, India. *Remote Sensing Applications: Society and Environment, 15*, 100239. https://doi.org/https://doi.org/10.1016/j.rsase.2019.100239.

Lacassin R, Devès M, Hicks S. P et al (2019). Rapid collaborative knowledge building via Twitter after significant geohazard events. *Geoscience Communication Discussions, 2019*, 1-23. https://doi.org/10.5194/gc-3-129-2020.

Mileti D. S, Cress D. M, Darlington J. D (2002). *Earthquake culture and corporate action.* Paper presented at the Sociological Forum. https://doi.org/10.1023/A:1014549708645.

Mileti D. S, Darlington J. D (1997). The role of searching in shaping reactions to earthquake risk information. *Social Problems, 44*(1), 89-103. https://doi.org/10.2307/3096875.

Momeni S, Madariaga R (2022). Long-term triggered seismicity on the Mosha fault by Damavand volcano, Iran: Implications on the seismic hazard of Tehran metropolis. *Frontiers in Earth Science, 10*, 945297. https://doi.org/10.3389/feart.2022.945297.

Mousavi, S.M., Beroza, G.C., (2023). Machine Learning in Earthquake Seismology. Annual Review of Earth and Planetary Sciences 51, 105–129. https://doi.org/10.1146/annurev-earth-071822-100323

Movaghari, R., and Javan Doloei, G. (2018). Upper Crustal Structure of South West of Tehran Using Borehole Ambient Noise Tomography. Journal of the Earth and Space Physics, 44(2), 281-295. DOI: https://dorl.net/dor/20.1001.1.2538371.1397.44.2.2.4

Nazari H, Ritz J.-F, Salamati R et al (2009). Morphological and palaeo-seismological analysis along the Taleghan fault (Central Alborz, Iran). *Geophysical Journal International, 178*(2), 1028-1041. https://doi.org/10.1111/j.1365-246X.2009.04173.x.

Nazeri S, Shomali Z. H (2019). Rapid estimation of the epicentral distance in the earthquake early warning system around the Tehran region, Iran. *Seismological Research Letters, 90*(5), 1916-1922. https://doi.org/10.1785/0220180375.

Niazpour, B., Shomali, Z. H. (2024). Moderate earthquakes striking Tehran metropolitan area: A case study of 2017 Malard and 2020 Damavand seismic sequences. *Journal of Seismology.* https://doi.org/10.1007/s10950-023-10187-z

Naserieh, S., Pakzad, M., Ghofrani, H., Dezvareh, M., Karkooti, E., Moradi, A., & Shahvar, M. (2023). Recognition of the causative fault of the 2017 MW 4.9 Malard (Tehran, Iran) earthquake from directivity analysis of the recorded ground motions. *Physics of the Earth and Planetary Interiors*, *345*, 107116. https://doi.org/10.1016/j.pepi.2023.107116

Oki T, Osaragi T (2017). Urban improvement policies for reducing human damage in a large earthquake by using wide-area evacuation simulation incorporating rescue and firefighting by local residents. *Planning Support Science for Smarter Urban Futures 15*, 449-468. https://doi.org/10.1007/978-3-319-57819-4_25.

Pedrami M (1981). Pasadenian orogeny and geology of last 700,000 years of Iran. *Geological Survey of Iranin*.

Priestley K, Baker C, Jackson J (1994). Implications of earthquake focal mechanism data for the active tectonics of the South Caspian Basin and surrounding regions. *Geophysical Journal International, 118*(1), 111-141. https://doi.org/10.1111/j.1365-246X.1994.tb04679.x.

Rashed T, Weeks J (2003). Assessing vulnerability to earthquake hazards through spatial multicriteria analysis of urban areas. *International Journal of Geographical Information Science, 17*(6), 547-576. https://doi.org/10.1080/1365881031000114071.

Ritz J.-F, Nazari H, Ghassemi A, Salamati R, Shafei A, Solaymani S, Vernant P (2006). Active transtension inside central Alborz: A new insight into northern Iran–southern Caspian geodynamics. *Geology, 34*(6), 477-480. https://doi.org/10.1130/G22319.1.

Ross Z. E, Trugman D. T, Hauksson E, Shearer P. M (2019). Searching for hidden earthquakes in Southern California. *Science, 364*(6442), 767-771. https://doi.org/10.1126/science.aaw6888.

Shabanian, E., & Hassanzadeh, M. A. (2022). Summary report on Quaternary/active faults in Tehran. https://www.researchgate.net/publication/384793110_Summary_report_on_Quaternaryactive_faults_in_Tehran

Shirzad T, Naghavi M, Afra M, Yamini-Fard F (2019). Three-dimensional P-wave velocity structure of Tehran from local micro-earthquake tomography. *Pure and Applied Geophysics, 176*, 4783-4796. https://doi.org/10.1007/s00024-019-02269-2.

SoltaniMoghadam S, Tatar M, Komeazi A (2019). An improved 1-D crustal velocity model for the Central Alborz (Iran) using Particle Swarm Optimization algorithm. *Physics of the Earth and Planetary Interiors, 292*, 87-99. https://doi.org/10.1016/j.pepi.2019.05.009.

Toomey, A., (2016). What happens at the gap between knowledge and practice? Spaces of encounter and misencounter between environmental scientists and local people. Ecology and Society 21. https://doi.org/10.5751/ES-08409-210228

Tchalenko J (1975). Seismotectonic framework of the North Tehran fault. *Tectonophysics, 29*(1-4), 411-420. https://doi.org/10.1016/0040-1951(75)90169-9.

Trifonov V, Hessami K, Jamali F (1996). West-Trending Oblique Sinitral—Reverse Fault system in Northern Iran: IIEES Special Publication 75. *Tehran, Iran*.

Vajedian S, Motagh M, Nilfouroushan F (2015). StaMPS improvement for deformation analysis in mountainous regions: Implications for the Damavand volcano and Mosha fault in Alborz. *Remote Sensing, 7*(7), 8323-8347.

Wang, X., Feng, X., Xu, X. *et al.* (2014). Fault plane parameters of Sanhe-Pinggu *M*8 earthquake in 1679 determined using present-day small earthquakes. *Earthq Sci* 27, 607–614. https://doi.org/10.1007/s11589-014-0099-3

Wetzler N, Lay T, Brodsky E. E (2023). Global Characteristics of Observable Foreshocks for Large Earthquakes. *Seismological Research Letters, 94*(5), 2313-2325. https://doi.org/10.1785/0220220397.

Yaghmaei-Sabegh S, Kun J, Qadri S. T (2023). Characteristics of records obtained at the 14 November 2021 Fin doublet events, Southern of Iran. *Natural hazards, 117*(1), 579-596. https://doi.org/10.1007/s11069-023-05873-7.

Yaghoob Nejad Asl N (2018). Vulnerability Assessment Caused by the Earthquake in Tehran and Surrounding Area. *Disaster Prevention and Management Knowledge (quarterly), 8*(1), 16-26.

Zare M (2020). Damavand quake: A trigger of risk panic in Tehran. *Journal of Disaster and Emergency Research*. https://doi.org/10.18502/jder.v3i2.3641.